

Catalysis Science & Technology

Accepted Manuscript



This article can be cited before page numbers have been issued, to do this please use: P. Hao, M. Zhang, W. Zhang, Z. Tang, N. Luo, R. Tan and D. Yin, *Catal. Sci. Technol.*, 2018, DOI: 10.1039/C8CY01191E.



This is an Accepted Manuscript, which has been through the Royal Society of Chemistry peer review process and has been accepted for publication.

Accepted Manuscripts are published online shortly after acceptance, before technical editing, formatting and proof reading. Using this free service, authors can make their results available to the community, in citable form, before we publish the edited article. We will replace this Accepted Manuscript with the edited and formatted Advance Article as soon as it is available.

You can find more information about Accepted Manuscripts in the [author guidelines](#).

Please note that technical editing may introduce minor changes to the text and/or graphics, which may alter content. The journal's standard [Terms & Conditions](#) and the ethical guidelines, outlined in our [author and reviewer resource centre](#), still apply. In no event shall the Royal Society of Chemistry be held responsible for any errors or omissions in this Accepted Manuscript or any consequences arising from the use of any information it contains.

Cite this: DOI: 10.1039/c0xx00000x

www.rsc.org/xxxxxx

ARTICLE TYPE

Polyoxometalate-based Gemini ionic catalysts for selective oxidation of benzyl alcohol with hydrogen peroxide in water

Pengbo Hao,[†] Mingjie Zhang,[†] Wei Zhang, Zhiyang Tang, Ni Luo, Rong Tan,* and Donghong Yin

Received (in XXX, XXX) Xth XXXXXXXXX 20XX, Accepted Xth XXXXXXXXX 20XX

DOI: 10.1039/b000000x

Keggin-type phosphotungstic acid (H₃PW₁₂O₄₀, HPW)-based *di*-imidazolium ionic liquid (IL) hybrids were prepared by exchanging the protons of HPW with PEG-bridged *di*-imidazolium cations in water. Characterization results suggested that intact Keggin-type [PW₁₂O₄₀]³⁻ anion was incorporated with various PEG-modified *di*-imidazolium cation through ionic interaction, giving PW-based ionic catalysts with Gemini structure. PEG-bridged *di*-imidazolium cations could not only fine-tune the redox properties of PW anions but also enhanced compatibility of catalyst in the aqueous system, which in turns improved the catalytic performance. Furthermore, combination of double catalytic sites into a single molecule enforced an intramolecular, cooperative reaction pathway resulting in further enhanced reaction rate and higher selectivity in selective oxidation of benzyl alcohol with H₂O₂ in water. More importantly, the *di*-imidazolium IL cations imparted reaction controlled phase-transfer function to the PW hybrids. The catalysts were thus precipitated from the aqueous system upon consumption of H₂O₂ and could be reused several times without loss of activity and selectivity.

Introduction

Benzaldehyde was an important chemical intermediate and raw material widely used in the manufacture of perfumes, agricultural chemicals, spices and other fine chemicals.¹⁻⁴ The conventional process for producing benzaldehyde is the hydrolysis of benzyl chloride.⁵ While, a trace amount of chlorine inevitably existed in the product, which didn't meet practical requirements for perfumery and the pharmaceutical industry. Liquid-phase oxidation of toluene and vapor-phase oxidation of benzyl alcohol were thus developed to produce chlorine-free benzaldehyde.⁶⁻⁹ But in the former process, the selectivity for benzaldehyde was rather low,^{10,11} and the latter process often requires high reaction temperatures, which resulted in high energy consumption, low selectivity for benzaldehyde, and deactivation of catalysts.¹² In view of these drawbacks of traditional synthesis methods, the liquid-phase oxidation of benzyl alcohol to benzaldehyde was more preferable, if it could be of low energy consumption, high selectivity for the desired product, and preventing catalyst deactivation. Hydrogen peroxide, which was cheap and mild for

the environment,¹³⁻¹⁵ was the ideal oxidant for this reaction undoubtedly from the viewpoint of green chemistry.

Polyoxometalates (POMs), a large family of bulky clusters of transition metal oxide with structural diversity, have received much attention in liquid-phase catalytic oxidation due to their controllable redox and acidic properties.¹⁶⁻²⁴ In particular, Keggin-type phosphotungstic acid (H₃PW₁₂O₄₀, HPW) have been revealed to be very effective in the selective oxidation of alcohols with aqueous H₂O₂.²⁵ However, pure POMs utilized in their bulk form had some drawbacks such as lower activity due to their very low surface area (<10 m² g⁻¹) and difficulty for catalyst recovery due to their water-solubility.²⁶ Immobilizing POMs onto supports with a large surface area ensured their enlarged surface area and facile recovery, but obtained heterogeneous HPW catalysts are often plagued by mass-transfer limitations during reactions.²⁷ Modification of POMs with organic units has been also applied to improve catalytic activity and reusability of POM catalysts,²⁸ since it could fine-tune the solubility and oxidizing capability of POM species. For example, Zhu' group reported a H₄PMo₁₁VO₄₀-based amphiphilic catalyst *via* functionalization of H₄PMo₁₁VO₄₀ by long alkyl chain-containing cationic surfactants.²⁹ They found that the amphiphilic characteristics of catalysts facilitated the access of organic benzyl alcohol to catalytic center, resulting in the enhanced catalytic activity for the selective oxidation of benzyl alcohol with aqueous H₂O₂. Unfortunately, the hydrophobic long alkyl chains in such hybrid hindered the interaction of H₂O₂ with POM to form active per-POM species. As a result, only moderate efficiency (60.6% of conversion) was observed over the amphiphilic catalyst in selective oxidation of benzyl alcohol with H₂O₂.

* Key Laboratory of Chemical Biology and Traditional Chinese Medicine Research (Ministry of Education); National & Local Joint Engineering Laboratory for New Petro-chemical Materials and Fine Utilization of Resources, Hunan Normal University, Changsha 410081 (P. R. China)

Fax: +86-731-8872531; Tel: +86-731-8872576; E-mail: yiyangtanrong@126.com

[†] These authors contributed equally to this work and should be considered co-first authors.

Room temperature IL with fascinating compatibility was an attractive organic modifier for POM.³⁰⁻³⁵ The inherent features, such as low volatility, large liquid ranges, and tunable polarity often promote the formation of hybrids with novel structures. Especially, the hybridization of ILs often transfers the ILs' properties to hybrids and fine-tunes their compatibility in heterogeneous system, which was very promising for their applications in heterogeneous catalysis.³⁶ *Di*-cationic imidazolium IL were known to allow the greater variety and control of ILs' virtual properties, including solubility and meltability.^{37, 38} Based on the fascinating features, we reasoned that the *di*-cationic IL could be used as the modifier for PW species and allowed for highly efficient catalyst for efficient selective oxidation of alcohols with aqueous H₂O₂. It was well known that the PW species had high negative charge and ability of forming salts, we thus decided to combine PW anions with IL cations through ionic interaction. Polyethylene glycol (PEG) with phase-transfer capability was employed to modify the IL cation, so as to further enhance the compatibility of catalyst and organic substrates for the aqueous oxidation. As expected, the Keggin-type [PW₁₂O₄₀]³⁻ anions were successfully coupled with the PEG-modified *di*-cationic imidazolium IL, giving PW-based ionic catalysts with Gemini structure. Combination of double catalytic sites into a single molecule enforced an intramolecular, cooperative reaction pathway resulting in enhanced reaction rates and higher selectivities in selective oxidation of benzyl alcohol with H₂O₂ in water. Furthermore, PEG-bridged *di*-imidazolium cations could not only fine-tune the redox properties of PW anions but also enhanced compatibility of catalyst in the aqueous system, further improving the catalytic performance of the PW-based ionic catalysts. More interestingly, the PW-based IL hybrids exhibited inverse dissolution-precipitation in water upon treatment with H₂O₂, which allowed for the homogeneous catalysis coupled with heterogeneous separation in the H₂O₂-based aqueous oxidation system. Activity switching was repeatable for seven cycles, which typically realized a homogeneous reaction coupled with heterogeneous separation in aqueous reactions.

Experimental

Materials and reagents

Keggin-type HPW was purchased from Macklin and used as received. *N*-methylimidazole was purchased from Alfa Aesar. Benzyl alcohol, 1-phenylethanol, cyclohexanol, 2-phenylethanol, diphenylmethanol and *n*-hexanol were purchased from Aladdin and used as received. Other commercially available chemicals were obtained from local suppliers. All of the solvents were purified by standard procedures before use. Other commercially available chemicals were laboratory-grade reagents obtained from local suppliers.

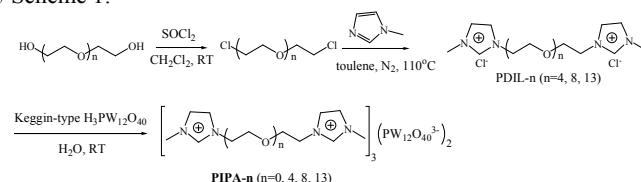
Methods

Fourier transform infrared (FT-IR) spectra were obtained from potassium bromide pellets with a resolution of 4 cm⁻¹ and 64 scans in the range of 400–4000 cm⁻¹ using an AVATAR 370 Thermo Nicolet spectrophotometer. The thermogravimetric and differential thermogravimetric (TG-DTG) curves were obtained on a NETZSCH STA 449C thermal analyzer. Samples (*ca.* 10 mg)

were heated from room temperature up to 800 °C was 10 K min⁻¹ under flowing air using alumina sample holders. Elemental analyses of C, H and N were carried out on a Vario EL III elemental analyser made in Germany. NMR spectra of samples were recorded on a BRUKER AVANCE -500 spectrometer. Powder X-ray diffraction (PXRD) pattern was scanned over a 2θ angle of 5° to 80° at an interval of 0.02°. X-ray Photoelectron Spectroscopy (XPS) data were obtained with a *K-Alpha*⁺ electron spectrometer from Thermo fisher Scientific using 300 W Al Kα radiation. Surface wettability of the samples was investigated by the analysis of the contact angles. The particle samples were directly pelletized without the aid of binders. A drop of DI water was placed on the pellet and imaged using a CCD camera (Fainstec, STC-GEC83A, Korea). Then, the contact angle was obtained by drawing a tangent. At least three measurements were carried out, and an averaged contact angle was taken. The content of tungsten in the samples was determined by inductively coupled plasma mass spectrometry (ICP-MS) on a NexION 300X analyzer (Perkin-Elmer Corp.). The reaction products were analyzed by a gas chromatograph (Agilent Technologies 6890N, HP-624 capillary column, 30 m × 0.25 mm) with flame ionization detector (FID) using nitrogen as the carrier gas. The products were identified by GC-MS using an HP 5790 series mass-selective detector.

Preparation of polyoxometalate-based Gemini ionic catalysts (PIPA-*n*, *n* = 0, 4, 8, 13, where *n* represented the repeated units number of ethylene oxide units in various PEG chains chains)

The Synthesis of PIPA-*n* (*n* = 0, 4, 8, 13) was outlined in Scheme 1.



Scheme 1 Synthesis of PIPA-*n* (*n* = 0, 4, 8, 13).

Preparation of PIPA-*n* (*n* = 4, 8, 13)

Synthesis of PEG-bridged *di*-imidazolium IL: polyethylene oxide-*n* (50 mmol, *n* = 4, 8, 13, which represented the degree of polymerization of polyethylene oxide) was mixed with pyridine (8 mL) in dichloromethane at room temperature. Thionyl chloride (110 mmol, 13.09 g) was then dropwise added into the solutions. The reaction mixtures were stirred at room temperature for 12 h under argon, and then concentrated in vacuum. Gummy residue was dissolved in ethyl acetate (50 mL) and filtrated to remove the insoluble salt of pyridinium chloride. Filtrate was concentrated in vacuum and further dried in vacuum at 40 °C overnight, giving viscous yellow liquid of chloride-terminated PEG-*n* (*n* = 4, 8, 13). The obtained chloride-terminated PEG-*n* (*n* = 4, 8, 13) (3 mmol) was mixed with 1-methyl imidazole (6.2 mmol, 0.51 g) in toluene (40 mL), and was refluxed at 110 °C for 48 h under argon protection. After removal of solvent, gummy residue was thoroughly rinsed with tetrahydrofuran and dried in vacuum to give a pale yellow viscous liquid of PEG-bridged *di*-imidazolium ILs (denoted as PDIL-*n*, *n* = 4, 8, 13). PDIL-4: FT-IR (KBr): $\gamma_{\max}/\text{cm}^{-1}$ 2921, 2866, 1736, 1650, 1538, 1459, 1354, 1297, 1249, 1109, 946, 845, 756, 665, 525. PDIL-8: FT-IR

(KBr): $\gamma_{\max}/\text{cm}^{-1}$ 2920, 2867, 1736, 1649, 1539, 1458, 1354, 1296, 1249, 1110, 947, 843, 756, 663, 524. PDIL-13: FT-IR (KBr): $\gamma_{\max}/\text{cm}^{-1}$ 2919, 2868, 1735, 1649, 1540, 1459, 1353, 1297, 1250, 1111, 947, 844, 757, 663, 525.

5 **Synthesis of PIPA-*n* (*n* = 4, 8, 13):** PEG-bridged *di*-imidazolium ILs (3 mmol) were mixed with Keggin-type HPW (2.1 mmol, 6.05 g) in water (50 mL). The mixture was stirred at room temperature for 48 h, resulting in white precipitate. After filtration, the resulting precipitate was collected, washed with
10 deionized water several times, and dried in vacuum overnight at room temperature, yielding **PIPA-*n*** (*n* = 4, 8, 13) as a white powder. **PIPA-4:** Calc. for $\text{C}_{54}\text{H}_{96}\text{N}_{12}\text{O}_{12}\text{P}_2\text{W}_{24}\text{O}_{80}$: C, 9.46; H, 1.41; N, 2.45%. Found: C, 9.35; H, 1.37; N, 2.57%. Tungsten content: 3.61 mmol/g (theoretical value: 3.50 mmol/g); ^1H NMR
15 (DMSO- d_6 , 500 MHz) δ_{H} , ppm: 9.04 (s, 2 H, ring N-CH₂-N), 7.68 (t, 4 H, ring -N-CH₂-CH₂), 7.65 (t, 4 H, ring -N-CH₂-CH₂), 3.52-3.57 (m, 16 H, CH₂-CH₂-O-CH₂-CH₂-O-CH₂-CH₂-), 1.24 (s, 6 H, ring -N-CH₃); FT-IR (KBr): $\gamma_{\max}/\text{cm}^{-1}$ 3149, 2971, 2883, 1079, 1050, 979, 895, 804, 625, 521. **PIPA-8:** Calc. for
20 $\text{C}_{78}\text{H}_{144}\text{N}_{12}\text{O}_{24}\text{P}_2\text{W}_{24}\text{O}_{80}$: C, 12.68; H, 1.96; N, 2.28%. Found: C, 12.71; H, 1.83; N, 2.19%. Tungsten content: 3.36 mmol/g (theoretical value: 3.25 mmol/g); ^1H NMR (DMSO- d_6 , 500 MHz) δ_{H} , ppm: 9.03 (s, 2 H, ring N-CH₂-N), 7.69 (t, 4 H, ring -N-CH₂-CH₂), 7.66 (t, 4 H, ring -N-CH₂-CH₂), 3.52-3.53 (m, 32 H, CH₂-CH₂-O-CH₂-CH₂-O-CH₂-CH₂-), 1.24 (s, 6 H, ring -N-CH₃); FT-
25 IR (KBr): $\gamma_{\max}/\text{cm}^{-1}$ 3150, 2969, 2884, 1079, 1049, 979, 895, 805, 625, 521. **PIPA-13:** Calc. for $\text{C}_{108}\text{H}_{204}\text{N}_{12}\text{O}_{40}\text{P}_2\text{W}_{24}\text{O}_{80}$: C, 16.08; H, 2.55; N, 2.08%. Found: C, 16.01; H, 2.38; N, 1.97%. Tungsten content: 2.69 mmol/g (theoretical value: 2.98 mmol/g); ^1H NMR
30 (DMSO- d_6 , 500 MHz) δ_{H} , ppm: 9.03 (s, 2 H, ring N-CH₂-N), 7.69 (t, 4 H, ring -N-CH₂-CH₂), 7.66-7.67 (t, 4 H, ring -N-CH₂-CH₂), 3.52-3.54 (m, 52 H, CH₂-CH₂-O-CH₂-CH₂-O-CH₂-CH₂-), 3.52 (m, 48 H, CH₂-CH₂-O-CH₂-CH₂-O-CH₂-CH₂-), 1.24 (s, 6 H, ring -N-CH₃); FT-IR (KBr): $\gamma_{\max}/\text{cm}^{-1}$ 3151, 2970, 2883, 1080,
35 1049, 979, 896, 805, 625, 522.

Preparation of PIPA-0

To evaluate the function of PEG moiety, a Gemini analog of PEG-free counterpart of **PIPA-0** in which ethyl group was employed as the linker, was prepared as a control catalyst. The
40 preparation procedure was similar to that of **PIPA-*n*** (*n* = 4, 8, 13), except for using 1,2-dichloroethane instead of chloride-terminated PEG to bridge 1-methylimidazole, as shown in Scheme 1. **PIPA-0.** Calc. for $\text{C}_{30}\text{H}_{72}\text{N}_{12}\text{P}_2\text{W}_{24}\text{O}_{80}$: C, 5.67; H, 1.14; N, 2.64%. Found: C, 5.84; H, 1.38; N, 2.39%. Tungsten
45 content: 3.64 mmol/g (theoretical value: 3.78 mmol/g); FT-IR (KBr): $\gamma_{\max}/\text{cm}^{-1}$ 3334, 3162, 2962, 1438, 1079, 1049, 979, 895, 805, 742, 625, 521.

Preparation of monomeric PW-based IL hybrids (denoted as IL-PW hybrid)

50 To elucidate the intramolecular, cooperative effect of Gemini structure of **PIPA-*n***, a mono-cationic counterpart of 1-methyl-3-butyl imidazolium phosphotungstate (denoted as IL-PW) was also prepared as a control catalyst by direct anion-exchange of 1-methyl-3-butylimidazolium chlorine (denoted as [BMIm]Cl) with
55 HPW. The structure of IL-PW hybrid was shown in Chart 1. Calc. for $\text{C}_{24}\text{H}_{54}\text{N}_6\text{PW}_{12}\text{O}_{40}$: C, 8.71; H, 1.63; N, 2.54%. Found: C,

8.59; H, 1.58; N, 2.37%. Tungsten content: 3.47 mmol/g (theoretical value: 3.63 mmol/g); FT-IR (KBr): $\gamma_{\max}/\text{cm}^{-1}$ 3150, 3108, 2962, 1565, 1460, 1160, 1079, 979, 895, 805, 625, 518.

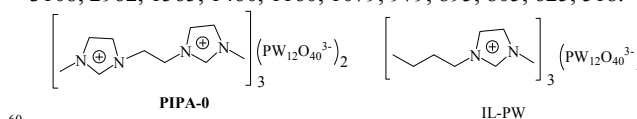


Chart 1 The structures of **PIPA-0** and **IL-PW**.

Catalyst testing

The PW-based catalyst (1.3 mol% of substrate, based on the
65 PW content) was mixed with benzyl alcohol (10 mmol) in deionized water (1.0 mL) under stirring. H₂O₂ (30 wt.%, 15 mmol) was diluted to the concentration of 10 wt.%, and then added dropwise to the above mixture within 1.5 h. The resulting mixture was stirred at 95 °C until the reaction was judged to be complete
70 based on GC analysis. After reaction, ethyl acetate (3 × 10 mL) was used to extract the products. Combined organic layers were dried with anhydrous Na₂SO₄. The products were analyzed by a gas chromatograph and further identified by GC-MS. PW-based catalyst was precipitated from the reaction system and separated
75 from the upper liquid phase by centrifugation. Being further washed with ethyl acetate and dried under vacuum, the recovered catalyst was used for the recycling experiment.

Results and discussion

Preparation of catalysts

80 Hybridization of POMs with IL units was an effective strategy to achieve POM-based hybrid catalysts with improved catalytic activity and convenient recovery, since the solubility and oxidizing capability of the obtained POM-based hybrids could be adjusted by the introduction of the organic moieties.³⁹ Different
85 from the common organic units (-NH₂ etc), IL as counteranion will transfer the ILs' properties to hybrids and fine-tune their compatible properties, which are very promising for the applications in the field of heterogeneous catalysis.^{36, 39} Especially, *di*-cationic imidazolium IL are known to allow the
90 greater variety and control of the ILs' vital properties, including solubility and meltability.⁴⁰ The fascinating advantages encouraged us to incorporate the Keggin-type HPW with *di*-imidazolium IL cation to achieve efficient and recoverable PW/IL hybrids for the selective oxidation of alcohols with H₂O₂ in water.
95 PEGs with phase-transfer capability were employed as the bridge of *di*-imidazolium IL cation, as so to further circumvent the mass transfer limitation of the aqueous oxidation.

The synthesis route for the PW/IL hybrids of **PIPA-*n*** (*n* = 4, 8, 13) was outlined in Scheme 1. PEG-bridged *di*-imidazolium
100 chlorine IL with various length of polyether linker was obtained by nucleophilic substitution of chloride-terminated PEG-*n* (*n* = 4, 8, 13) with *N*-methylimidazole under alkaline condition. Successive anion-exchange with Keggin-typed HPW allowed for the incorporation of *di*-imidazolium cation with PW anion
105 through ion interaction. The approach gave PW-based IL hybrids of **PIPA-*n*** (*n* = 4, 8, 13) with Gemini structure. For comparison, a PEG-free counterpart of **PIPA-0**, in which an ethyl group was acted as the bridge, was also prepared according to a similar procedure, except for the use of 1,2-dichloroethane instead of

chloride-terminated PEG, as shown in Scheme 1.

Unlike the pristine HPW that is soluble in water, the obtained **PIPA-n** ($n = 0, 4, 8, 13$) were insoluble in water, as shown by the typical **PIPA-8** (Fig. 1A). The change in solubility indicated successful incorporation of PW ion with PEG-based IL. Interestingly, it formed water-soluble active species by the action of H_2O_2 during oxidation (Fig. 1B); and returned to insoluble when H_2O_2 was used up (Fig. 1C). The H_2O_2 -induced inverse water-solubility made **PIPA-n** behave as reaction controlled phase-transfer catalysts for the selective oxidation of alcohols with aqueous H_2O_2 in water.

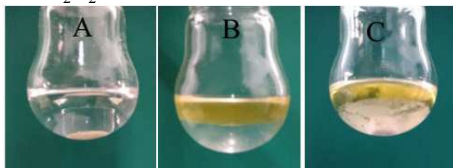


Fig. 1 Photographs of **PIPA-8**-mediated oxidation of benzyl alcohol with H_2O_2 in water (Before reaction (A); during reaction (B); after reaction (C)). Reaction conditions: Catalyst (1.3 mol% substrate, based on the PW loading), benzyl alcohol (10 mmol), water (1.5 ml), H_2O_2 (30 wt.%, 15 mmol), 95 °C, 6 h.

Characterization of Samples

FT-IR

FT-IR spectrum was used to identify structural and bonding changes in **PIPA-n** hybrids. **PIPA-8** with a middling length of PEG spacer was chose as the typical hybrid for the structural identification. Fig. 2 showed the FT-IR spectra of pristine Keggin-type HPW, PEG-bridged *di*-imidazolium chlorinum IL of PDIL-8, **PIPA-8** and **PIPA-8** (reused for seven times) hybrids. Clearly, Keggin-type HPW showed characteristic P-O_a stretching (1079 cm^{-1}), W=O_d terminal stretching (990 cm^{-1}), stretching of W-O_c-W inter bridges between corner-sharing WO₆ octahedra (895 cm^{-1}), and stretching of W-O_e-W intra bridges between edge-sharing WO₆ octahedra (805 cm^{-1}) in FT-IR spectrum (Fig. 2a).⁴¹ Notably, these characteristic bands remained in FT-IR spectrum of **PIPA-8**, in spite of a slight shift (Fig. 2c vs. 2a). It suggested the incorporation of intact Keggin-typed PW anion in **PIPA-8** hybrid. Red shift of W=O_d band from 990 to 979 cm^{-1} confirmed the presence of ionic interaction between imidazolium IL cation and PW anion upon the hybridization.^{42, 43} Furthermore, for the hybrid, the single P-O_a at 1079 cm^{-1} split into three bands at 1079 and 1049 cm^{-1} (Fig. 2c). It might attribute to the formation of hydrogen bonding between terminal oxygen atoms of PW anions and the hydrogen atoms (-N-C(H)₂-N-) in imidazolium ring.^{42, 43} Indeed, the C-H stretch modes in imidazole ring (at 625 cm^{-1}) also exhibited a split upon hybridization due to the participation of hydrogen bond (Fig. 2c vs. 2b). The results demonstrated that Keggin-type PW anion was coupled with PEG-bridged *di*-imidazolium IL cations in **PIPA-8** through ionic interaction together with hydrogen bond. In addition, we noticed that a new band at 947 cm^{-1} appeared as a branch of the band at 979 cm^{-1} (W=O_d) in FT-IR spectrum of **PIPA-8**. It was reported to be the reduced W⁵⁺ species.^{43, 44} Therefore, W⁶⁺ species coexisted with low valent W⁵⁺ species in the typical hybrid of **PIPA-8**. The observation provided direct evidence that the combined imidazolium IL cation adjusted the redox property of W species in **PIPA-8**, which in turn fine-tuned

55 catalytic activity of the PW-based catalyst.

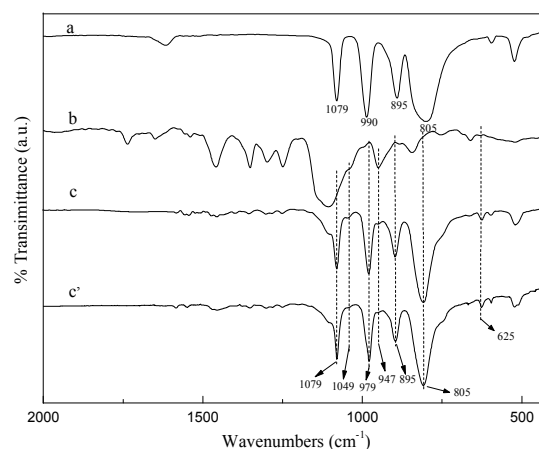


Fig. 2 FT-IR spectra of Keggin-type HPW (a), PDIL-8 (b), **PIPA-8** (c), and **PIPA-8** reused for seven times (c').

XPS

XPS provided further evidence for adjusting redox property of W species by *di*-imidazolium cation in **PIPA-8**. Fig. 3 showed the XPS of pure HPW and **PIPA-8**. As expected, pure HPW exhibited only O1s (associated with physisorbed and structural water in HPW), P2p, and W4f peaks in the XPS survey spectrum (Fig. 3A). New C1s (284.6 eV) and N1s (400.2 eV) signals appeared in XPS survey spectrum of **PIPA-8**. It suggested the incorporation of organic *di*-imidazolium cation with Keggin PW anion. Notably, the combination resulted in an increase in the binding energy of W⁶⁺ (W4f_{7/2} and W4f_{5/2}) from 36.17 and 38.33 eV to 36.44 and 38.59 eV, respectively (Fig. 3B). Increased binding energy verified electronic interactions between the *di*-imidazolium cations and PW anion. Redox property of W species could thus be fine-tuned by the combined imidazolium IL cation. Indeed, low valent W⁵⁺ species was coexisted with W⁶⁺ species in **PIPA-8**, as evident from the appearance of new peak at ca. 34.9 eV in W4f XPS spectrum (Fig. 3B). These results strongly indicated the partial reduction of W⁶⁺ species in the PW moiety of **PIPA-8**, which arisen from the intermolecular electronic interactions between the PEG-bridged *di*-imidazolium cations and the Keggin PW anion.

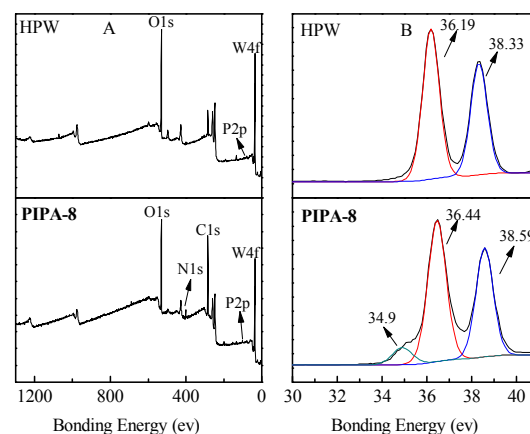


Fig. 3 XPS survey spectra (A) and W4f XPS spectra (B) of HPW and **PIPA-8**.

UV-vis

UV-vis DR spectra provides an evidence for the intermolecular electronic interactions between the PEG-bridged *di*-imidazolium cations and the Keggin PW anion. As shown in Fig. 4, pristine Keggin-type HPW exhibited three absorption peaks at 216, 258 and 322 nm (Fig. 4a). They were assigned to $O_a^{2-} \rightarrow P^{5+}$ charge-transfer transition, $O^2- \rightarrow W^{6+}$ charge transfer where W atoms were located in $W-O_c-W$ intra bridges between edge-sharing WO_6 octahedra, and $O^2- \rightarrow W^{6+}$ charge transfer where W atoms were located in $W-O_c-W$ inter bridges between corner-sharing WO_6 octahedra, respectively.⁴¹ For PW/IL hybrid of **PIPA-8**, the $O^2- \rightarrow W^{6+}$ charge transfer peak at 322 nm blue-shifted to 296 nm (Fig. 4b vs. 4a), which could be attributed to the presence of ionic and hydrogen bond interactions between PW anion and imidazolium cations.^{41, 45} The other two absorptions remain at the same energy upon the hybridization (Fig. 4b vs. 4a). We could thus deduce that the only O^2- atoms which were located in $W-O_c-W$ inter bridges between corner-sharing WO_6 octahedra participated in the electronic interaction. Notably, the typical **PIPA-8** exhibited absorption band associated with reduced W^{5+} species at 505 nm (see Fig. 4 inset curve a). And the band was undetectable for pristine Keggin-type HPW (see Fig. 4 inset curve b). The observation further confirmed the existence of strong interaction between cations and anions, which finely adjusted the redox properties of W species.

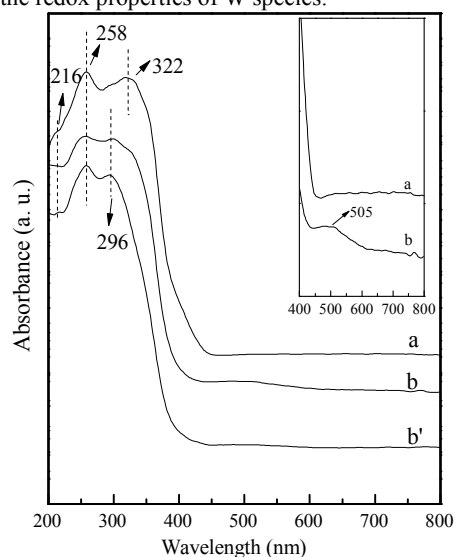


Fig. 4 UV-Vis DR spectra of Keggin-type HPW (a), **PIPA-8** (b) and **PIPA-8** reused for seven times (b'). Inset shows the enlarged UV-Vis DR spectra of Keggin-type HPW (a) and **PIPA-8** (b) in the range of 400–800 nm.

TG-DTG

Thermogravimetric analysis (TGA) further verified the incorporation of *di*-imidazolium IL cation with PW anion through electronic interaction, as shown in Fig. 5. Pristine Keggin-type HPW showed three distinct steps of weight loss at 74, 178 and 421 °C in the combined TG-DTG curves, when it was heated from room temperature to 800 °C under airflow (Fig. 5A). The first weight loss was due to the removal of physisorbed water (a variable amount depending on the number of hydration waters in the sample). The second weight loss accounted for the removal of

crystallization water, which were hydrogen-bonded to the acidic protons to form the $[H_2O \cdot \cdot H^+ \cdot \cdot OH_2]$ ions. And the third weight loss resulted from the removal of all acidic protons from the anhydrous $H_3PW_{12}O_{40}$. It corresponded to loss of constitutional water to form an anhydride phase $PW_{12}O_{38.5}$.⁴⁶ Notably, such loss of physical adsorbed and structural water was not observed in the case of **PIPA-8** hybrid below 200 °C (Fig. 5B). It was speculated that the hydrophobicity of **PIPA-8** reduced the adsorbed water in the composite material, and the crystallization water should be also nonexistent due to the absence of acidic protons in the hybrid. The observations suggested the removal of structural water and three protons during the assembly of HPW with PEG-bridged imidazolium IL. Similar results were discussed in the previous reports.⁴⁵ Above 200 °C, the organic part (PEG-bridged imidazolium cation) in **PIPA-8** begin to decompose, and the sharp loss in weight (*ca.* 13 wt.%) was appeared at 226 °C. Notably, the initial decomposition temperature of organic part significantly decreased as compared with that in PDIL-8 which exhibited the decomposition at 322 °C (Fig. 5B vs. 5C). The decrease in decomposition temperature should be probably due to that bulky PW cations increased the distance between cationic PEG-bridged imidazolium moieties in the hybrids, which thus reduced thermal stability of the organic part. Further weight loss in the temperature range of 407–649 °C (*ca.* 8.0 wt.%) could be assigned to the decomposition of the remaining organic part, and /or the destroyed of the Keggin structure. The decomposition was complete at about 649 °C to form the constituent oxides P_2O_5 and WO_3 . TGA analysis revealed that the content of organic moiety in **PIPA-8** was *ca.* 21 wt.% (0.40 mmol g^{-1}). PW content could thus be estimated to be *ca.* 0.27 mmol g^{-1} in the **PIPA-8** hybrid, which approximate to the content of the $PW_{12}O_{40}^{3-}$ moiety (0.263 mmol g^{-1}) calculated from ICP-MS result (3.36 mmol/g of tungsten content).

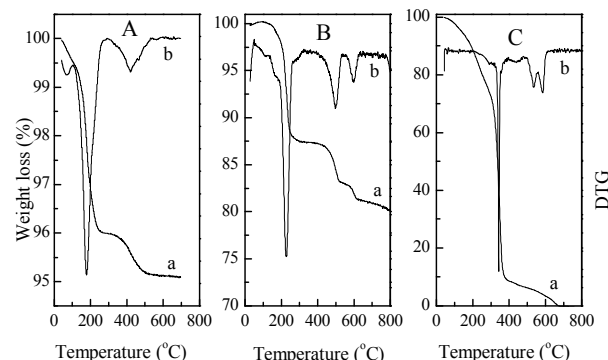


Fig. 5 TG-DTG curves of pristine Keggin-type HPW (A), **PIPA-8** hybrid (B) and PDIL-8 (C) ((a) thermogravimetric curves; (b) differential thermogravimetric curves).

SEM

SEM images gave direct information of the hybridization of *di*-imidazolium cations with PW anions, as well as the morphologies of corresponding hybrids, as shown in Fig. 6. Obviously, pristine Keggin-type HPW exhibited bulk form with very low surface area (Fig. 6a). Combining the bulk HPW with *di*-imidazolium IL resulted in the formation of uniform particle (*ca.* 650 nm) with a regular cubic shape (Fig. 6b). The great difference in morphology confirmed the hybridization of bulk HPW with *di*-imidazolium IL.

Notably, introducing various PEG moieties in the imidazolium IL cations didn't significantly affect the hybridization behavior of **PIPA-n**, since **PIPA-n** ($n=4, 8, 13$) gave a similar morphology to **PIPA-0** (Fig. 6c–e vs. 6b). We could thus deduce that the hybridization process was only triggered by the electronic interaction between *di*-imidazolium cations and PW anions, independent of the PEG linkers.

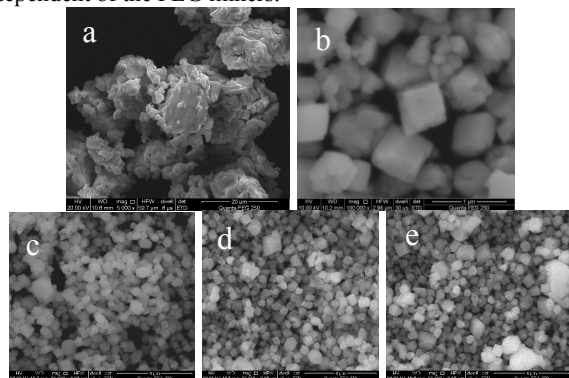


Fig. 6 SEM images of pristine Keggin-type HPW (a), **PIPA-0** (b), **PIPA-4** (c), **PIPA-8** (d), and **PIPA-13** (e)

PXRD

PXRD was used to further study the change in structure of PW during the hybridization process. The wide-angle PXRD patterns of pristine Keggin-type HPW and the typical **PIPA-8** were shown in Fig. 7.

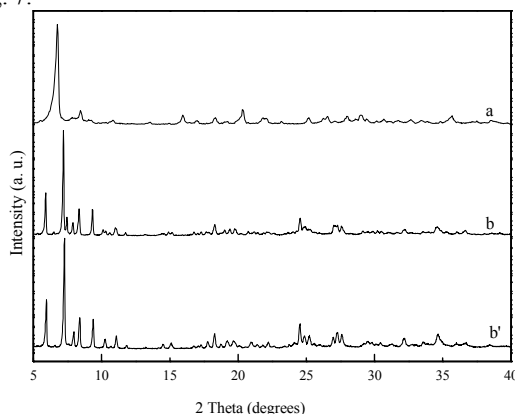


Fig. 7 PXRD patterns of pristine Keggin-type HPW (a), **PIPA-8** (b) and **PIPA-8** reused for seven times (b').

Obviously, a set of sharp Bragg peaks, characteristic of Keggin-type HPW, were obvious in the PXRD pattern of neat HPW (Fig. 7a). While, all these peaks disappeared in the case of **PIPA-8**, despite the preservation of Keggin structure of PW species upon the hybridization (Fig. 7a vs. 7b). Concomitantly, a novel set of well-resolved diffraction peaks appeared in the PXRD pattern of **PIPA-8** (Fig. 7a vs. 7b). The observations suggested that Keggin-type HPW was successfully incorporated with the *di*-imidazolium IL through ionic interactions, as well as hydrogen bonding, giving rise to a different crystal structure. The particle size of **PIPA-8** could be quantitatively evaluated from the XRD data using the Debye–Scherrer equation, $D = k\lambda/\beta\cos\theta$, which gave a relationship between peak broadening in XRD and particle size. In this equation D was the thickness of the crystal, k was the Debye–Scherrer constant (0.89), λ was the X-ray wavelength

(0.154184 nm) and β was the line broadening in radian obtained from the full width at half maximum, θ was the Bragg angle. According to the Debye–Scherrer equation, we could calculate the average size of **PIPA-8** was 685 nm. This result was in agreement with the SEM image for **PIPA-8** shown in Fig. 6.

Water contact angle (WCA) measurement

The wettability of **PIPA-n** ($n=0, 4, 8, 13$) was studied by means of static WCA measurements (Fig. 8). The WCA value of **PIPA-0** was ca. 131°, implying the hybrid was hydrophobic (Fig. 8A). After PEG modification, WCA value became smaller (56–80°), implying the **PIPA-n** ($n=4, 8, 13$) became hydrophilic (Fig. 8B–8D). Considering the amphiphilic of PEG modifier, it was concluded that the wettability transformation of **PIPA-n** ($n=0, 4, 8, 13$) was essentially originated from PEG linker of polyoxometalate-based Gemini ionic catalysts. Indeed, the WCA value of **PIPA-n** ($n=4, 8, 13$) increased as the length of polyether chain increased (Fig. 8B vs. 8C vs. 8D). The various wettability would directly affect the inherent phase transfer capability of **PIPA-n** ($n=0, 4, 8, 13$), and further their catalytic efficiency in oxidation of benzyl alcohol in water.

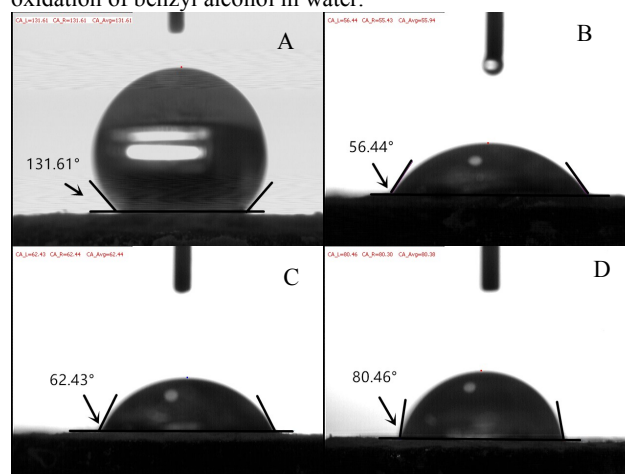


Fig. 8 Contact angle measurements of **PIPA-0** (A), **PIPA-4** (B), **PIPA-8** (C) and **PIPA-13** (D).

Catalytic performances

Since benzaldehyde was a very important carbonyl compound for widespread applications, catalytic performances of the **PIPA-n** ($n=0, 4, 8, 13$) were evaluate in selective oxidation of benzyl alcohol to benzaldehyde in water using aqueous H_2O_2 (30 wt.%) as an oxidant. The results were summarized in Table 1. To demonstrate the positive effect of *di*-cationic imidazolium IL on catalytic performance, the mono-cationic counterpart of IL-PW hybrid was prepared as the control catalyst by electrostatic coupling of PW anion with 1-methyl-3-butyl imidazolium cation. The Keggin-type HPW was also used for comparison.

Obviously, pure HPW showed low catalytic efficiency in the aqueous selective oxidation of benzyl alcohol with H_2O_2 (30 wt.%) due to poor accessibility of hydrophobic substrate to water-soluble active site in water. Only 48% conversion of the benzyl alcohol with moderate selectivity (67%) was observed in spite of the water-solubility of HPW (Table 1, entry 1). Mono-cationic IL-PW hybrid offered higher conversion of 59% (Table 1, entry 3) and selectivity (80%) than the neat HPW under identical reaction conditions, although the counter IL of [BMIm]Cl was inactive

(Table 1, entry 2). It indicated the efficient tuning of the redox properties of W species by the imidazolium IL cation. Moreover, it couldn't be excluded that the compatible imidazole-based IL cation may favor the adsorption of the benzyl alcohol molecule and thus enhanced the activity. However, the mono-cationic IL-PW hybrid was far less active than the *di*-cationic IL-based **PIPA-n** ($n=0, 4, 8, 13$) (Table 1, entry 3 vs. entries 4–7). Using aqueous H_2O_2 as oxygen source, the *di*-cation IL-based **PIPA-0** gave higher conversions (71%) and selectivity (82%) in the selective oxidation of benzyl alcohol with aqueous H_2O_2 (30 wt.%) in water (Table 1, entry 4). The reason for higher efficiency of **PIPA-n** might be the *di*-cationic structure of imidazolium IL. It could couple with trivalent PW anions at a molar ratio of 3: 2. Multiple catalytic PW sites were thus combined into the formed hybrid through the ionic self-assembly route,⁴⁷ enforcing an intramolecular, cooperative reaction pathway. Incorporating a phase-transfer PEG group into the *di*-imidazole-based IL linker further improved the catalytic efficiency (Table 1, entries 5–7). The higher activity of **PIPA-n** ($n=4, 8, 13$) should be related with the built-in phase transfer capability of **PIPA-n** arisen from PEG modifier. Actually, amphiphilic characteristics of PEG moiety not only improved the solubility of organic substrate in the aqueous reaction, but also enhanced interaction of H_2O_2 with PW anion to form PW_4 species that was the real active catalyst in the selective oxidation.⁴⁸

Table 1 Results of the selective oxidation of alcohols to aldehydes with H_2O_2 in water over various PW-based catalysts^a

Entry	Catalyst	Substrates	Products	Conv. (%) ^b	Sel. (%) ^c
1	HPW			48	67
2	[BMIm]Cl			Trace	/
3	IL-PW			59	80
4	PIPA-0			71	82
5	PIPA-4			88	79
6	PIPA-8			91	84
7	PIPA-13			96	86
8	HPW			48	>99
9	IL-PW			70	>99
10	PIPA-13			95	>99
11	HPW			43	>99
12	IL-PW			82	>99
13	PIPA-13			95	>99
14	HPW			37	>99
15	IL-PW			56	>99
16	PIPA-13			74	>99
17	HPW			4	61
18	IL-PW			7	90
19	PIPA-13			12	89

20	HPW			5	57
21	IL-PW			9	75
22	PIPA-13			17	78

^a) Catalyst (1.3 mol% substrate, based on the PW loading), substrates (10 mmol), water (1.5 ml), H_2O_2 (30 wt.%, 15 mmol), 95 °C, 6 h.

^b) Conversion was based on alcohols.

^c) Selectivity was based on the corresponding aldehydes or ketones.

To further understand the advantages of enhanced cooperative catalysis, as well as built-in phase transfer capability, for **PIPA-n** ($n=0, 4, 8, 13$) in the aqueous oxidation, kinetics was thus used to study the reaction rates of aqueous selective oxidation of benzyl alcohol over **PIPA-0**, **PIPA-4**, **PIPA-8**, **PIPA-13**, and mono-cationic IL-PW hybrid in detail. The corresponding kinetic curves and rate curves are shown in Fig. 9. Clearly, benefiting from the Gemini structure, **PIPA-n** ($n=0, 4, 8, 13$) afforded higher efficiency than the mono-counterpart of IL-PW (Fig. 9a-d vs. 9e). Although it also has a *di*-cationic structure, **PIPA-0** was far less active than **PIPA-n** ($n=4, 8, 13$) as evidenced by the lower conversion of benzyl alcohol (Fig. 9A-d vs. 9A(a-c)) and reduced K_{obs} (Fig. 9B-d vs. 9B(a-c)). This observation demonstrated that inherent phase transfer capability of **PIPA-n** ($n=4, 8, 13$) arisen from PEG linker was favored in the catalysis. Indeed, the length of PEG spacer was found to influence reaction rates of the aqueous selective oxidation of benzyl alcohol. **PIPA-13** showed the highest catalytic efficiency, giving almost quantitative conversion (96%) of benzyl alcohol within 6 h (Fig. 9a). Further shortening the bridged polyether chain led to a decreased activity in the reaction accordingly (Fig. 9b and 9c). A possible explanation might be that the length of polyether chain directly affected not only the inherent phase transfer capability of catalyst, but also the cooperative interaction of the bridged active sites. Although increasing the total length of PEG spacer reduced the phase transfer capability of catalysts, it might enhance the flexibility of the bulky PW species, and thus improved the intramolecular cooperation resulting in enhanced reaction rates. Therefore, **PIPA-13** with the longest length of PEG spacer presented here gave highest overall activity in the selective oxidation of benzyl alcohol in water.

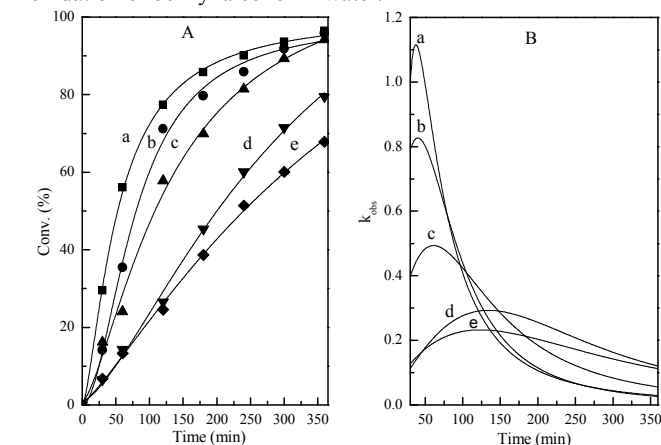


Fig. 9 Kinetic curves (A) and rate curves (B) of selective oxidation of benzyl alcohol over **PIPA-13** (a), **PIPA-8** (b), **PIPA-4** (c), **PIPA-0** (d), and IL-PW (e) in water.

Remarkable enhancement of reaction rates with the employment of the **PIPA-13** was also observed in the case of 1-phenylethanol, cyclohexanol, diphenylmethanol, 2-phenylethanol, and *n*-hexanol, as shown by their conversions in Table 1 (Table 1, entry 10 vs. entries 8 and 9, entry 13 vs. entries 11 and 12, entry 16 vs. entries 14 and 15, entry 19 vs. entries 17 and 18, entry 22 vs. entries 20 and 21). Conversions of the corresponding alcohols were dependent on the nature of substrates used in this work. Secondary alcohols, such as 1-phenylethanol and cyclohexanol, were readily oxidized in water using aqueous H₂O₂ as oxidant, giving corresponding ketones with high yields (95%) (Table 1, entries 10 and 13). Diphenylmethanol underwent a slower oxidation over **PIPA-13** due to unfavorable accessibility of bulky substrate to active sites (Table 1, entry 16). Primary aliphatic alcohols, such as 2-phenylethanol and 1-hexanol (Table 1, entries 19 and 22), were far less reactive than the secondary alcohols (Table 1, entries 10, 13, and 16) and also the benzyl alcohol (Table 1, entry 7). The conversions were less than 17% when 1.5-fold molar excess of H₂O₂ was used (Table 1, entries 19 and 22).

Superiority of **PIPA-13** over other reported PW-based hybrids, such as self-assembled *IL*-PW hybrid ([PyHA]₃PW and [TMGOH]_{2.2}H_{0.8}PW),⁴⁹ *IL*-modified SBA-15 supported PW catalyst (PW-NH₂-*IL*-SBA-15),⁵⁰ and MCM-41 supported PW catalyst ((PW)₃/MCM-41)⁵¹ was seen in Table 2. Obviously, **PIPA-13** was more efficient than these reported PW-based hybrids either homogeneous or heterogeneous in oxidation of benzyl alcohol with H₂O₂ in water (Table 2, entry 1 vs. entries 2-5). Notably, although PW-NH₂-*IL*-SBA-15 had a similar countered imidazolium *IL* cation, it required 3-fold molar excess of H₂O₂ to afford the yield of benzaldehyde (83%) equal to that over **PIPA-13** (Table 2, entry 4 vs. 1). Furthermore, the *IL*-free hybrid of (PW)₃/MCM-41 gave only 20% yield of benzaldehyde even with 3-fold molar excess of H₂O₂ (Table R1, entry 5). Higher efficiency of **PIPA-13** demonstrated the advantages of built-in phase transfer capability, as well as enhanced cooperative action, for the PW-based Gemini ionic catalyst in the aqueous oxidation.

Table 2 Comparison of results obtained over different catalysts in the selective oxidation of benzyl alcohol with H₂O₂^a

Entry	Catalyst	Reaction time (h)	Mol ratio (H ₂ O ₂ /alcohol)	Yield ^b (%)	Ref
1	PIPA-13	6	1.5	83	This work
2	[TMGOH] _{2.2} H _{0.8} PW	6	1.5	81	Ref. ^c
3	[PyHA] ₃ PW	6	1.5	70	Ref. ^c
4	PW-NH ₂ - <i>IL</i> -SBA-15	6	3.0	83	Ref. ^d
5	(PW) ₃ /MCM-41	18	3.0	20	Ref. ^e

a) Catalyst (1.3 mol% substrate, based on the PW loading), substrates (10 mmol), water (1.5 ml), H₂O₂ (30 wt.%, 15 mmol), 95 °C, 6 h.

b) Determined by GC.

c) Data from the Ref.⁴⁹

d) Data from the Ref.⁵⁰

e) Data from the Ref.⁵¹

It should be more attractive if the activity and structural integrity of **PIPA-n** (n = 4, 8, 13) was preserved during the aqueous oxidation at 95 °C. ³¹P NMR was employed to

investigate the stability of typical **PIPA-13** hybrid during the reaction (Fig. 10). **PIPA-13** hybrid exhibited distinct P signal of [PW₁₂O₄₀]³⁻ at -15.1 ppm in ³¹P NMR spectrum (Fig. 10a). The P signal gradually disappeared as reaction progress accompanied by the appearance of signal associated with [PW₄O₈(O₂)₈]³⁻ species at -0.9 ppm (Fig. 10b-e). The distinguishing change suggested the partial degradation of [PW₁₂O₄₀]³⁻ into peroxy-bridged [PW₄O₈(O₂)₈]³⁻ species by the reaction with H₂O₂. The resulting [PW₄O₈(O₂)₈]³⁻ species was water-soluble and acted as the real active species for catalyzing alcohols oxidation. With the consumption of H₂O₂, the soluble [PW₄O₈(O₂)₈]³⁻ species transformed into the insoluble Keggin-type [PW₁₂O₄₀]³⁻ species, as evident from the reappeared [PW₁₂O₄₀]³⁻ signal at -15.1 ppm (Fig. 10e). Notably, the [PW₄O₈(O₂)₈]³⁻ signal in ³¹P NMR almost disappeared, and only the signal associated with [PW₁₂O₄₀]³⁻ existed after the complete consumption of H₂O₂ at 6 h (Fig. 10f). We thus propose that the [PW₁₂O₄₀]³⁻ species was recovered after the reaction, and the water-insolubility of catalyst ensured it to be facilely separated from the aqueous system for reuse.

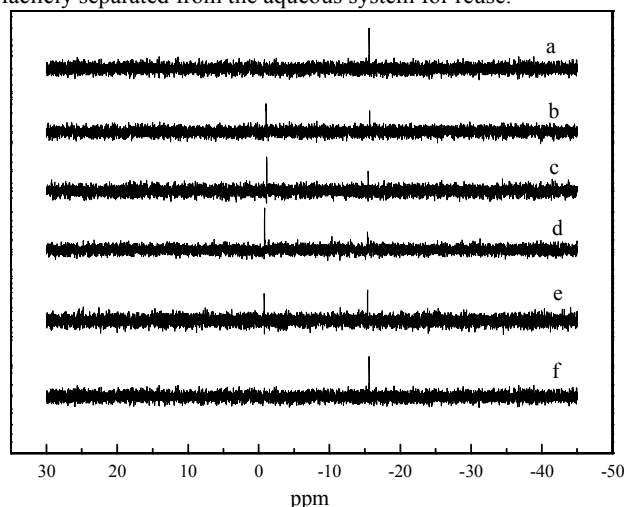


Fig. 10 Changes in ³¹P NMR spectra of **PIPA-13** in selective oxidation of benzyl alcohol with H₂O₂ in water: before reaction (a), the reaction after 1 h (b), 2 h (c), 3 h (d), 5 h (e), and 6 h (f).

Indeed, the **PIPA-n** (n = 4, 8, 13) could be almost quantitatively (>99%) recovered from the reaction mixture by centrifugation. Fig. 11 showed the reusability of **PIPA-n** (n = 4, 8, 13) hybrids in selective oxidation of benzyl alcohol to benzaldehyde with H₂O₂ in water. As expected, all the hybrids could be reused for seven times with no appreciable decrease in activity and selectivity of benzaldehyde, which demonstrated their excellent stability. ICP-MS analysis of recovered typical **PIPA-8** gave an almost identical content of tungsten element (3.19 mmol/g) to that of the fresh one (3.36 mmol/g). Furthermore, a negligible amount of soluble active species could be detected in the filtrate in terms of tungsten percentage according to ICP-MS analysis. FT-IR (Fig. 2c vs. 2c') and UV-vis spectra (Fig. 4b vs. 4b') gave direct evidence of the stability of **PIPA-n** (n = 4, 8, 13) based on the fact that no significant change in typical **PIPA-8** occurred even after reusing seven times. Furthermore, PXRD analysis indicated that the structural integrity of **PIPA-8** was well-preserved during the reaction, since crystallinity of **PIPA-8** was well retained after the recyclability test (Fig. 7b vs. 7b'). The observations demonstrated the perfect

stability of the PIPA-*n* (*n* = 4, 8, 13) catalysts in the H₂O₂-mediated oxidation system without degradation and leaching.

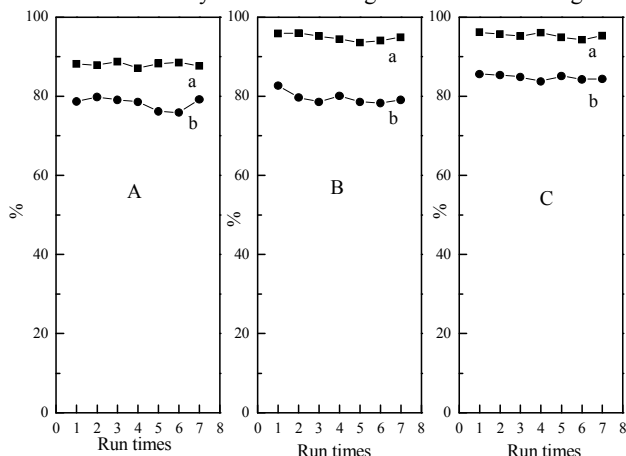


Fig. 11 Reusability of PIPA-4 (A), PIPA-8 (B) and PIPA-13 (C) in the selective oxidation of benzyl alcohol with H₂O₂ as an oxidant (a: conversion; b: selectivity).

Conclusions

We have developed novel PW-based ionic hybrids by anion-exchanging PEG-functionalized *di*-imidazolium IL cations with Keggin PW-anions. The *di*-imidazolium IL cations endowed the PW catalysts with some distinct characteristics as follows: (a) dense active sites for cooperative catalysis; (b) high compatibility in water; (c) built-in phase transfer capability for aqueous oxidation. The new PW-based catalysts thus exhibited excellent catalytic efficiency, convenient recovery and steady reuse in the liquid-phase oxidation of alcohols to corresponding aldehydes with aqueous H₂O₂ (30 wt.%) in water. Salient advantages of the PW-based ionic hybrids inspired us to develop more versatile POM-based catalysts for heterogeneous H₂O₂-based organic oxidations in water.

Acknowledgements

This work was supported by the National Natural Science Foundation of China (21676078, 21476069), the Natural Science Foundation of Hunan Province for Distinguished Young Scholar (2016JJ1013) and the Talents Foundation of Key Laboratory of Chemical Biology and Traditional Chinese Medicine Research (KLCBTCMR201703).

References

- M.N. Grayson, Z. Yang, K.N. Houk, *J. Am. Chem. Soc.*, 2017, **139**, 7717.
- X. Chen, E.J. Sorensen, *J. Am. Chem. Soc.*, 2018, **140**, 2789.
- P. Šafář, Š. Marchalín, M. Šoral, J. Moncol, A. Daich, *Org. Lett.*, 2017, **19**, 4742.
- Y. Wang, P. Ren, X. Gu, X. Wen, Y. Wang, X. Guo, E.R. Waclawik, H. Zhu, Z. Zheng, *Green Chem.*, 2016, **18**, 1482.
- G.D. Yadavand, B.V. Haldavanekar, *J. Phys. Chem. A*, 1997, **101**, 36.
- S.S. Acharyya, S. Ghosh, R. Tiwari, B. Sarkar, R.K. Singha, C. Pendem, T. Sasaki, R. Bal, *Green Chem.*, 2014, **16**, 2500.
- S. Ghosh, S.S. Acharyya, D. Tripathi, R. Bal, *J. Mater. Chem. A*, 2014, **2**, 15726.
- S. Kitano, A. Tanaka, K. Hashimoto, H. Kominami, *Phys. Chem. Chem. Phys.*, 2014, **16**, 12554.

- A. Kumar, V.P. Kumar, A. Srikanth, V. Vishwanathan, K.V.R. Chary, *Catal. Lett.*, 2016, **146**, 35.
- X. Li, X. Wang, M. Antonietti, *ACS Catal.*, 2012, **2**, 2082.
- J. Lv, Y. Shen, L. Peng, X. Guo, W. Ding, *Chem. Commun.*, 2010, **46**, 5909.
- W. Yi, W. Yuan, Y. Meng, S. Zou, Y. Zhou, W. Hong, J. Che, M. Hao, B. Ye, L. Xiao, Y. Wang, H. Kobayashi, J. Fan, *ACS Appl. Mater. Inter.*, 2017, **9**, 31853.
- B. Martin, J. Sedelmeier, A. Bouisseau, P. Fernandez-Rodriguez, J. Haber, F. Kleinbeck, S. Kamptmann, F. Susanne, P. Hoehn, M. Lanz, L. Pellegatti, F. Venturoni, J. Robertson, M.C. Willis, B. Schenkel, *Green Chem.*, 2017, **19**, 1439.
- H.W. Kim, M.B. Ross, N. Kornienko, L. Zhang, J. Guo, P. Yang, B.D. McCloskey, *Nat. Catal.*, 2018, **1**, 282.
- M. Borrell, M. Costas, *J. Am. Chem. Soc.*, 2017, **139**, 12821.
- Y. Ma, H. Peng, J. Liu, Y. Wang, X. Hao, X. Feng, S.U. Khan, H. Tan, Y. Li, *Inorg. Chem.*, 2018, **57**, 4109.
- S. Thanasilp, J.W. Schwank, V. Meeyoo, S. Pengpanich, M. Hunsom, *J. Mol. Catal. A: Chem.*, 2013, **380**, 49.
- F. Mirante, L. Dias, M. Silva, S.O. Ribeiro, M.C. Corvo, B. de Castro, C.M. Granadeiro, S.S. Balula, *Cata. Comun.*, 2018, **104**, 1.
- J.A.F. Gamelas, F. Oliveira, M.G. Evtugina, I. Portugal, D.V. Evtuguin, P.D.V. Evtuguin, *Appl. Catal. A: Gen.*, 2016, **509**, 8.
- C.M. Granadeiro, A.D.S. Barbosa, P. Silva, F.A.A. Paz, V.K. Saini, J. Pires, B. de Castro, S.S. Balula, L. Cunha-Silva, *Appl. Catal. A: Gen.*, 2013, **453**, 316.
- D. Long, E. Burkholder, L. Cronin, *Chem. Soc. Rev.*, 2007, **36**, 105.
- C. Wu, M. Zhao, *Adv. Mater.*, 2017, **29**, 1.
- M. Blasco-Ahicart, J. Soriano-López, J.J. Carbó, J.M. Poblet, J.R. Galan-Mascaros, *Nat. Chem.*, 2017, **10**, 24.
- Z. Min, Z. XianWei, W. ChuanDe, *ACS Catal.*, 2017, **7**, 6573.
- X. Dong, X. Zhang, P. Wu, Y. Zhang, B. Liu, H. Hu, G. Xue, *ChemCatChem.*, 2016, **8**, 3680.
- G.S. Kumar, M. Vishnuvarthan, M. Palanichamy, V. Murugesan, *J. Mol. Catal. A: Chem.*, 2006, **260**, 49.
- V.N. Panchenko, I. Borbáth, M.N. Timofeeva, S. Göbölös, *J. Mol. Catal. A: Chem.*, 2010, **319**, 119.
- J. Tong, W. Wang, L. Su, Q. Li, F. Liu, W. Ma, Z. Lei, L. Bo, *Catal. Sci. Technol.*, 2017, **7**, 222.
- L. Jing, J. Shi, F. Zhang, Y. Zhong, W. Zhu, *Ind. Eng. Chem. Res.*, 2013, **52**, 10095.
- K. Dong, X. Liu, H. Dong, X. Zhang, S. Zhang, *Chem. Rev.*, 2017, **117**, 6636.
- M. Zhang, W. Zhu, H. Li, S. Xun, W. Ding, J. Liu, Z. Zhao, Q. Wang, *Chem. Eng. J.*, 2014, **243**, 386.
- D. Julião, R. Valença, J.C. Ribeiro, B. de Castro, S.S. Balula, *Appl. Catal. A: Gen.*, 2017, **537**, 93.
- S. Herrmann, L. De Matteis, J.M. de la Fuente, S.G. Mitchell, C. Streb, *Angew. Chem. Int. Edit.*, 2017, **56**, 1.
- Y. Gong, Q. Hu, C. Wang, L. Zang, L. Yu, *Langmuir*, 2016, **32**, 421.
- G. Gilbert F. De, P. Raquel, V. Charles, E. Xabier, L. Jalel, H. Jason P., W. Tom, *ACS Sustain. Chem. Eng.*, 2016, **4**, 6031.
- H.G.O. Alvim, T.B. de Lima, H.C.B. de Oliveira, F.C. Gozzo, J.L. de Macedo, P.V. Abdelnur, W.A. Silva, B.A.D. Neto, *ACS Catal.*, 2013, **3**, 1420.
- J.L. Anderson, R. Ding, A. Ellern, D.W. Armstrong, *J. Am. Chem. Soc.*, 2005, **127**, 593.
- I.M. Gindri, D.A. Siddiqui, C.P. Frizzo, M.A.P. Martins, D.C. Rodrigues, *ACS Appl. Mater. Inter.*, 2015, **7**, 27421.
- X. Chen, B. Souvanhthong, H. Wang, H. Zheng, X. Wang, M. Huo, *Appl. Catal. B: Environ.*, 2013, **138-139**, 161.
- R. Wang, C.M. Jin, B. Twamley, J.M. Shreeve, *Inorg. Chem.*, 2006, **45**, 6396.
- T. Rajkumar, G.R. Rao, *Mater. Lett.*, 2008, **62**, 4134.
- Y. Leng, J. Wang, D. Zhu, M. Zhang, P. Zhao, Z. Long, J. Huang, *Green Chem.*, 2011, **13**, 1636.
- L. Yan, P. Zhao, M. Zhang, J. Wang, *J. Mol. Catal. A: Chem.*, 2012, **358**, 67.
- J.C. Duhacek, D.C. Duncan, *Inorg. Chem.*, 2007, **46**, 7253.
- G. Rao, T. Rajkumar, B. Varghese, *Solid State Sci.*, 2009, **11**, 36.

- 46 L. Zhang, K. Su, J. Ming, Z. Li, B. Cheng, *Adv. Mater. Res.*, 2011, **233**, 58.
- 47 Y. Gong, Q. Hu, C. Wang, L. Zang, L. Yu, *Langmuir*, 2016, **32**, 421.
- 48 S. Zhang, G. Zhao, S. Gao, Z. Xi, J. Xu, *J. Mol. Catal. A: Chem.*, 2008, **289**, 22.
- 5 49 G. Chen, Y. Zhou, Z. Long, X. Wang, J. Li, J. Wang, *ACS Appl. Mater. Interfaces*, 2014, **6**, 4438
- 50 R. Tan, C. Liu, N. Feng, J. Xiao, W. Zheng, A. Zheng, D. Yin, *Microporous and Mesoporous Mater.*, 2012, **158**, 77.
- 10 51 S. Singh, A. Patel, *Catal. Lett.*, 2016, **146**, 1059.

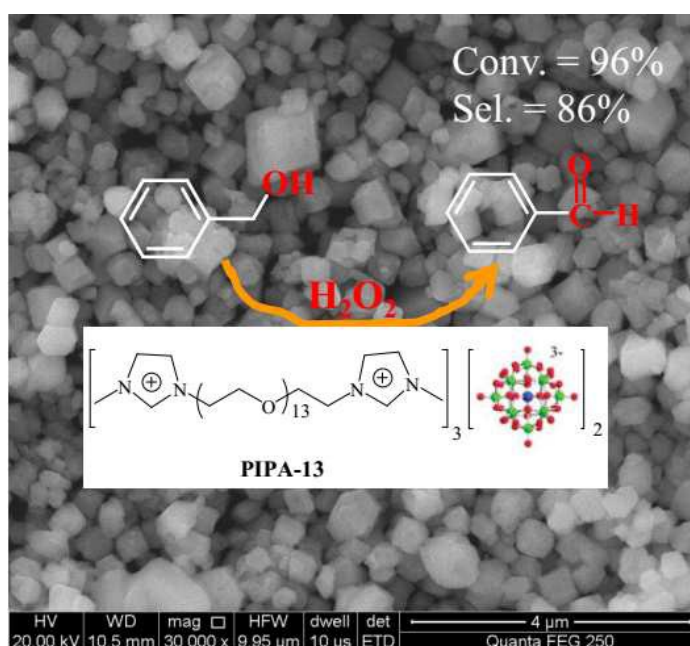
Graphical Abstract

Polyoxometalate-based Gemini ionic catalysts for selective oxidation of benzyl alcohol with hydrogen peroxide in water

Pengbo Hao, Rong Tan^{*}, Mingjie Zhang, Wei Zhang, Zhiyang Tang, Ni Luo and Donghong Yin

National & Local Joint Engineering Laboratory for New Petro-chemical Materials and Fine Utilization of Resources, Key Laboratory of Chemical Biology and Traditional Chinese Medicine Research (Ministry of Education), Hunan Normal University, Changsha 410081, P. R. China.

Polyoxometalate-based Gemini ionic hybrids with inherent phase-transfer capability are the highly efficient and recyclable catalysts in the selective oxidation of alcohols with H₂O₂ in water.



^{*} Corresponding authors. Fax: +86-731-8872531. Tel: +86-731-8872576

E-mail: yiyangtanrong@126.com